International Journal of Food Science +Technology

Institute of Food Science +Technology ifst

Original article

Rapid screen of aflatoxin-contaminated peanut oil using Fourier transform infrared spectroscopy combined with multivariate decision tree

Yu Yang,[1] Yanan Zhang,[1] Caiyan He,[1] Mengyuan Xie,[1] Huitai Luo,[2] Ying Wang[3]* & Jun Zhang[14]*

1 Key Laboratory of Optoelectronic Information and Sensing Technologies of Guangdong Higher Education Institutes, Jinan University, 601 Huangpu Ave. West, Guangzhou 510632, China
2 Guangdong Provincial Key Laboratory of Emergency Test for Dangerous Chemicals, Guangdong Provincial Public Laboratory of Analysis and Testing Technology, Guangdong Institute of Analysis, Building 34, 100 Xianlie Middle Road, Guangzhou 510070, China
3 Department of Food Science and Engineering, College of Science and Engineering, Jinan University, 601 Huangpu Ave. West, Guangzhou 510632, China
4 State Key Laboratory of Applied Optics, Changchun Institute of Optics, Fine Mechanics and Physics, Chinese Academy of Sciences, Changchun 130033, China

(Received 26 March 2018; Accepted in revised form 8 May 2018)

Summary Contamination of peanut oil is a great concern in the industry. FTIR spectroscopy combined with chemometrics could develop a rapid and nondestructive method to screen aflatoxin-contaminated peanut oil. Aflatoxin B1 (AFB1)- and aflatoxin (AFT)-positive peanut oils were screened by mid-IR (MIR) with classification models established by a novel multivariate decision tree (MDT) method. Two discriminant functions were developed in the fingerprint region based on absorbance ratio and moving window Fisher discrimination analysis methods for the two complex nodes in each MDT model. Window adjustment reduced the total different spectral data points in modelling to 23. The true-positive and true-negative rate of calibration and validation could both reach up to 100%. These results would render the possibility of efficient and economical design of a portable high-speed multitasking MIR instrument for screening AFB1- and AFT-contaminated peanut oil.

Keywords Aflatoxin, aflatoxin B1, mid-IR, multivariate decision tree, peanut oil.

Introduction

Global peanut oil production was in ascending trend over the last few years and achieved 5.89 million tons in 2016. China, European Union and the United States were the major importers and exporters, contributing to around 90% of the world's trade in 2016. Among which China was the largest importer and exporter, accounting for over half of the global market (United States Department of Agriculture, 2017).

Aflatoxins (AFTs), produced naturally by *Aspergillus flavus* and *Aspergillus parasiticus* (Ayres *et al.*, 1971), are a notorious hazard in peanut oil, nuts, maize, *etc.* (Liu *et al.*, 2011; Lee *et al.*, 2015). AFTs are well-known carcinogenic, teratogenic, mutagenic and immunosuppressive agent. They are sequential of derivatives of coumarin and dihydrofuran with similar chemical structures (Clifford & Rees, 1967). The double furan ring in their molecule contributes to their toxicity (Ayres *et al.*, 1971). There are fourteen different types of AFTs (AFB1, AFB2, AFG1 and AFG2 are the major ones), and AFB1 is the most toxic one and accounts for most of the AFTs (Boutrif, 1998). Different countries have established different regulations on the maximum content of AFTs, AFB1 or both in food and feed. China sets the regulation limit at 20 ppb for AFB1 in peanut oil (National Health and Family Planning Commission of the People's Republic of China & China Food and Drug Administration, 2017). Peanut oil containing less than 20 ppb AFTs is also considered safe by the U.S. Food and Drug Administration (Korani *et al.*, 2017).

High-performance liquid chromatography (HPLC) (Daradimos *et al.*, 2000), liquid chromatography–tandem mass spectrometry (LC-MS/MS) (De Santis *et al.*,

*Correspondent: Fax: +8620-85226630;
e-mail: twangywy@jnu.edu.cn (YW) and Fax: +8620-85220420;
e-mail: 472969511@qq.com (JZ)

doi:10.1111/ijfs.13831

2017), MALDI TOF mass spectrometry (Ramos Catharino *et al*., 2005), FRET-based fluorescence immunoassay (Zekavati *et al*., 2013), electrokinetic capillary chromatography (Holland & Sepaniak, 1993) and enzyme-linked immunosorbent assay (Yang *et al*., 2009) have been used to determine AFB and AFG contents. Extraction and isolation of AFTs in these methods are labour-intensive, time-consuming, invasive to samples, usually performed in the laboratory and require large amount of organic solvents (Tripathi & Mishra, 2009; Zhang *et al*., 2014).

Near IR (NIR) spectroscopy and mid-IR (MIR) spectroscopy have been combined with chemometrics to detect AFB1 and AFTs in samples through the developed models in quantitative and qualitative analysis. These methods required less detection time and preparation time, which could save solvents, samples and cost. In quantitative analysis, partial least-squares (PLS) regression has usually been combined with IR to evaluate the content of AFB1 in paddy rice (Zhang *et al*., 2014), red chilli powder (Tripathi & Mishra, 2009), *etc*., and the content of AFTs in maize (Lee *et al*., 2015), peanut paste (Kaya-Celiker *et al*., 2014), *etc.,* through the developed regression models. However, PLS regression could bring false-negative and false-positive results in prediction intervals of AFB1/AFTs content, which is not a risk in qualitative analysis (Montgomery, 2013; Brereton, 2015).

In qualitative analysis, NIR spectra have been combined with forward feature selection (FFS)-linear discriminant classifier, FFS-quadratic discriminant classifier (Durmuş *et al*., 2017), PLS-DA (Fernández-Ibañez *et al*., 2009), *etc.,* to diagnose AFB1-/AFT-positive figs, maize and barley through the developed classification models. More than 1000 spectral data points in NIR spectra were employed to extract principal features in the above studies for AFB1/AFTs. Broader, weaker and more overlapped absorption bands were presented by NIR spectra compared with MIR spectra. In MIR spectra, around 350–520 data points in fingerprint regions could also achieve it, when combined with principal component analysis (PCA)-DA (Kaya-Celiker *et al*., 2014), linear discriminant analysis (Lee *et al*., 2015), PCA-k nearest neighbour analysis (Shen *et al*., 2016), etc.

So far, none of the IR analytical techniques has been explored to detect AFB1-/AFT-positive peanut oil. MIR spectra could record more recognisable characteristic bands of the contaminated peanut oil. Multivariate decision tree (MDT) classification method could work well in generating important insights based on these characteristic bands and interpreting those (Kamiński *et al*., 2018). Reduction of data points in classification models would facilitate the design of portable high-speed MIR instruments more efficiently and economically. Therefore, the objectives of this study were to assess the feasibility of MIR technique to screen AFB1- and AFT-positive peanut oil develop efficient classification models using a novel MDT algorithm with less data points involved and evaluate their efficiency and predictive accuracy for unknown samples. Findings of this study will build models that can be incorporated in the design of portable high-speed multitasking MIR instruments for a real-time monitoring and high-throughput screening with cost advantage.

Materials and methods

Preparation of the contaminated peanut oil samples

The AFT-contaminated samples were produced using the general AFTs induction methods (Fernández-Ibañez *et al*., 2009; Kaya-Celiker *et al*., 2014). About 5 kg peanuts, purchased from a local retailer, were placed in a humidity chamber and the humidity was set to 85% at 27 °C to induce the growth of AFTs. About 35 g incubated peanuts were picked randomly, pressed and filtered through a cotton sieve to obtain a peanut oil sample of about 10 mL (Suihua automatic oil press, ZY-70, Guangdong, CN). Three samples were produced in alternate days, and 90 AFT-contaminated oil samples were collected within 60 days. In this study, samples were classified as AFB1-/AFTs (AFB1, AFB2, AFG1 and AFG2)-positive when the content of AFB1/AFTs was higher than 20 ppb and AFB1-/AFT-negative if the content of AFB1/AFTs was less than 20 ppb.

Determination of AFB1 and AFTs contents

The chemical contents of AFB1 and AFTs in the samples were provided by China national analytical centre (Guangdong Institute of analysis). They were determined using LC-MS/MS (Agilent 1200 SL Series RRLC/6410B Triple Quard MS, USA), following GB 5009.22-2016 (National Health and Family Planning Commission of the People's Republic of China & China Food and Drug Administration, 2016).

MIR spectra acquisition

A FTIR spectrometer (Nicolet iS50, Thermo Fisher Scientific, Guangdong, CN) equipped with an all-reflection diamond attenuated total reflectance (ATR) crystal accessory and a proprietary DL-α-alanine doped triglycine sulphate (DLaTGS) detector was used to obtain the spectra of the oil samples. MIR spectra were collected in the range of 4000 to 650 cm^{-1} at a resolution of 4 cm^{-1} with 32 scans for each sample at room temperature. A background spectrum was obtained against air before each measurement. All the measurements were done in triplicate and the average

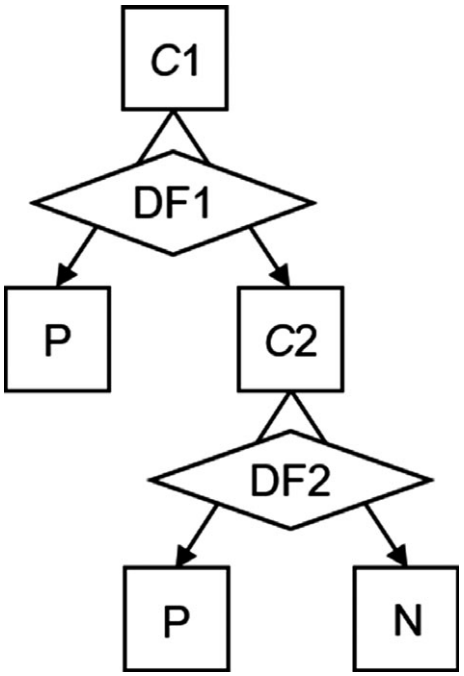

Figure 1 Multivariate decision tree for screening of peanut oil samples. P-positive; N-negative.

spectrum was reported. The cleaning of ATR crystal was done before each measurement.

Statistical methods

The chemical content of each sample in calibration set was used to classify positive or negative group, which was categorical dependent variable. Calculated statistics from the corresponding spectra were used as independent variables. Both dependent and independent variables were used to develop AFB1-MDT and AFTs-MDT classification models. Each node in a MDT model represents a class label denoted as a positive-node, negative-node or complex-node (*C*1 or *C*2) (Fig. 1). The branches of a complex-node were formed based on the discriminant function (DF). Absorbances at multiple wavenumbers in the selected spectral region were used in the DF establishment. DF1 was generated by absorbance ratio (AR) and DF2 was generated by moving window Fisher discriminant analysis (MWFDA) methods in MDT model as shown in Fig. 1. Each sample in validation set could be assigned to either positive or negative by plugging its spectra into established MDT model. True-positive rate (TPR) measures the proportion of positives that are correctly identified as such. True-negative rate (TNR) measures the proportion of negatives that are correctly identified as such (Zweig & Campbell, 1993). TPR and TNR were used to evaluate the performance of MDT model. Two MDT models were both established on MATLAB R2016b software (The MathWorks, Inc., MA, USA) for AFB1 and AFTs. Eighteen out of ninenty oil samples were randomly chosen as the validation set and not subjected to the modelling process. The remaining seventy two oil samples were used as the calibration set. For AFB1-MDT modelling, AFB1 contents were 2–635 ppb (seven AFB1-negative and eleven AFB1-positive) in validation set and 2–2497 ppb (twenty AFB1-negative and fifty-two AFB1-positive) in calibration set. For AFTs-MDT modelling, AFTs contents were 2–982 ppb (five

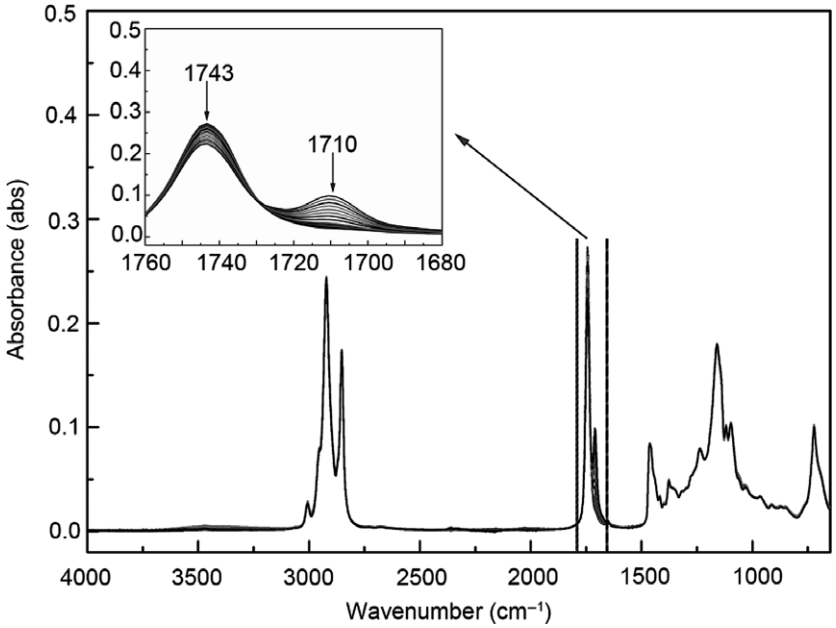

Figure 2 MIR spectra of peanut oil samples; the inset plot shows an enlarged version of the spectra in the region of 1760–1680 cm^{-1}.

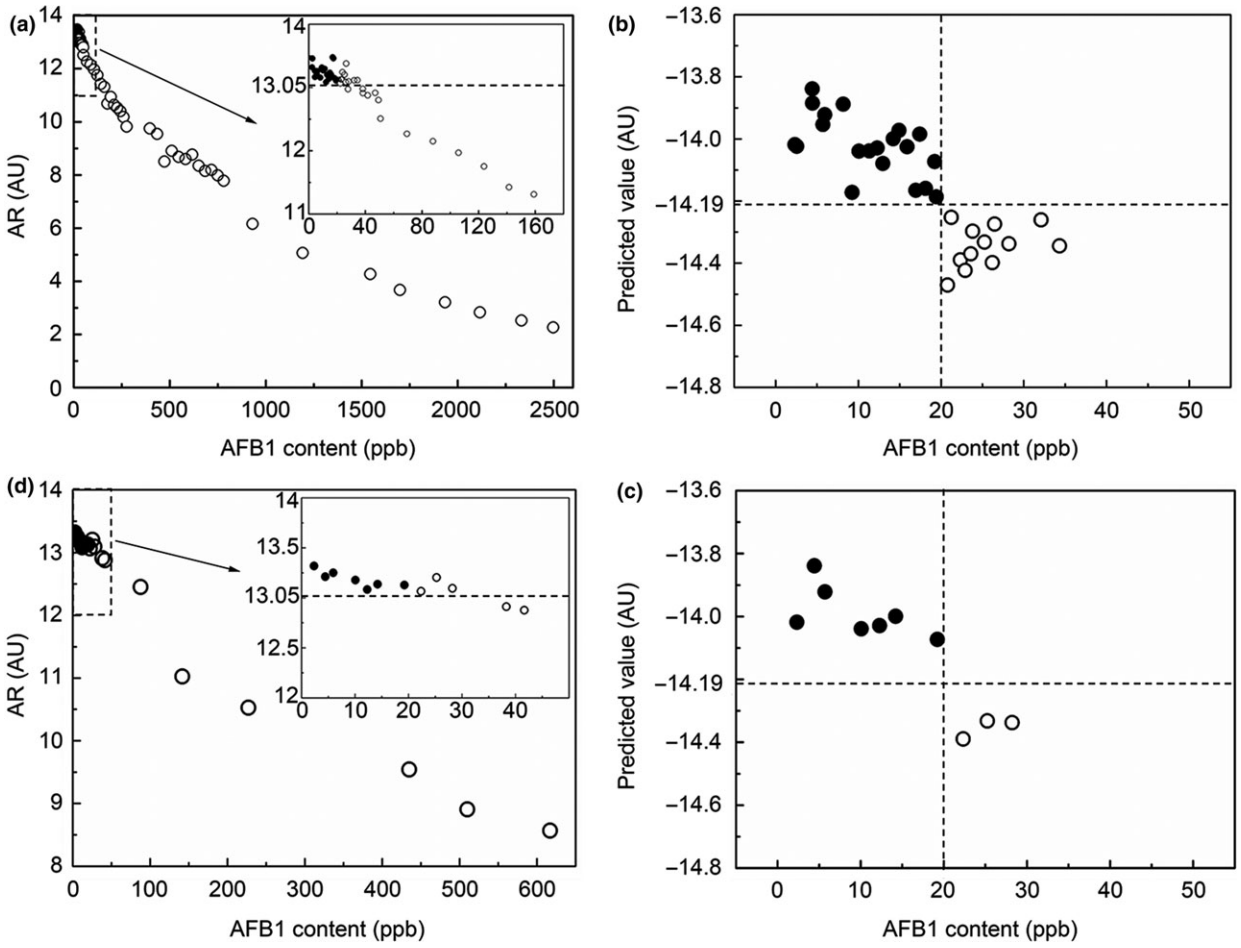

Figure 3 DF1 and DF2 classification results of MDT model in calibration (a and b) and validation (c and d) for AFB1. Positive samples denoted by open circles; negative samples denoted by filled circles.

AFT-negative and thirteen AFT-positive) in validation set and 2–3699 ppb (twelve AFT-negative and sixty AFT-positive) in calibration set.

Generation of discrimination function 1

Absorbance ratio method has been used to detect compositional differences in order to identify waste cooking oil, determinate degree of deacetylation in chitin and distinguish AFTs contamination higher than 100 ppb in single corn kernel (Shigemasa *et al.*, 1996; Pearson *et al.*, 2001; Huang *et al.*, 2016). ARDF was expressed as follows:

$$f(a_i, a_j) = \begin{cases} \mathrm{P}, & \frac{a_i}{a_j} < \mathrm{AR}_{\mathrm{threshold}} \\ C2, & \text{otherwise,} \end{cases} \quad (1)$$

where a_i and a_j were absorbances at selected representative wavenumber i and j, respectively. P was positive, and $\mathrm{AR}_{\mathrm{threshold}}$ was the decision threshold of the ARDF. Averages of each pair of adjacent AR values were plotted to find the $\mathrm{AR}_{\mathrm{threshold}}$ maximising TPR with no negative miscarriage. ARDF was used to be the DF1 for the $C1$-node in MDT to screen highly contaminated AFB1-/AFT-positive samples (Fig. 1).

Generation of discrimination function 2

Fisher discriminant analysis method could classify samples based on a linear discriminant function (LDF) of spectral features in selected spectral wavebands (Li *et al.*, 2003). It was an effective tool used in spectral pattern recognition (Diniz *et al.*, 2014; Durmuş *et al.*, 2017). The LDF was expressed as follows:

$$f(A) = \begin{cases} \mathrm{P}, & \sum_{i=1}^{n} \omega_i a_i < \omega_{\mathrm{threshold}} \\ \mathrm{N}, & \text{otherwise,} \end{cases} \quad (2)$$

where data set $A = [a_1, a_2, \ldots, a_n]$, n was the number of spectral data points, ω_i was weight factor of a_i (i = 1, 2, …, n), $\omega_{\mathrm{threshold}}$ was the decision threshold of the

LDF, P was positive, N was negative. ω_i and $\omega_{threshold}$ were determined based on the principle of maximising the ratio of between-class variance and minimising the ratio of within-class variance (Li *et al*., 2003).

Moving window (MW) technique was combined with FDA method to develop the LDFs in all windows of selected spectral wavebands. Windows of various sizes moved over the region with the moving distance as one wavenumber. The optimal LDF (OLDF) was obtained when its corresponding window contained minimum spectral data points, and its TPR and TNR were closest to 1. OLDF was used to be the DF2 in MDT model for the *C*2-node to screen the rest of AFB1-/AFT-positive samples (Fig. 1).

Results and discussion

Interpretation of MIR spectra

Mid-IR spectrum reflected the molecular structure information of peanut oil, AFTs and their source fungi in oil samples. All spectra looked very similar (Fig. 2). Bands around 3475 cm^{-1}, at 3008, 2922 and 2853 cm^{-1}, at 1743 cm^{-1} and 1710 cm^{-1}, at 1465 cm^{-1} and 1377 cm^{-1}, around 1237–1033 cm^{-1}, at approximately 1237–1033 cm^{-1}, at around 965 and 915 cm^{-1}, at 722 cm^{-1} were observed in all the spectra. The oil samples were mainly glycerol esters of different fatty acids, and the highly unsaturated molecules in the complex might lead to characteristic bands in the same regions (Fennema, 1997; Kaya-Celiker *et al*., 2014). The above bands could be contributed to the overtone of the glyceride ester carbonyl absorption, C=C-H *cis*-stretching, asymmetric and symmetric C-H stretching modes of the methylene groups, the C=O group of triglycerides and dicarboxylic monoesters in oxidation products, the scissoring band of the bending vibration of the methylene group and symmetrical bending vibration of the methyl groups, asymmetric coupled vibrations of C-C (=O)-O and O-C-C, C=C-H out of plane bending vibration of *trans*- and *cis*-disubstituted olefins, the combination of rocking and the out of plane bending vibrations of *cis*-disubstituted olefin (Sinclair *et al*., 1952; Fennema, 1997; Guillén & Cabo, 1997; Pinto *et al*., 2010; Karunathilaka *et al*., 2017).

With the increase in AFTs (AFB1) contamination, decrease in the absorbance around 1743 cm^{-1} and increase in the absorbance around 1710 cm^{-1} were observed (Inset in Fig. 2). Fungi could break lipids down into FFA and partial glycerides. Absorption around 1743 cm^{-1} and 1710 cm^{-1} were due to ester linkage in oil and dicarboxylic monoesters produced from cleavage and oxidation of free fatty acids (FFA) following oil hydrolysis, respectively. These wavebands could be used to represent the fungal deterioration (Sinclair *et al*., 1952; Fennema, 1997; Kaya-Celiker *et al*., 2014).

Bands belonging to absorption of the functional groups of AFTs were not observed. Absorbance bands of the relative small amount of AFTs might have been overlapped by those of the oil, as suggested by Kaya-Celiker *et al*. (2014).

The spectral absorption at waveband of 1760–1680 cm^{-1} was obviously different from those at other spectral sections and changed with contamination intensity. Therefore this waveband was selected as the fingerprint region to develop classification models.

AFB1-MDT model calibration and validation

Absorbances of 1743 cm^{-1} and 1710 cm^{-1} in the fingerprint region were selected as a_i and a_j in (1), respectively. AR was reversely proportional to AFB1 content corresponding to the increasing absorbance at

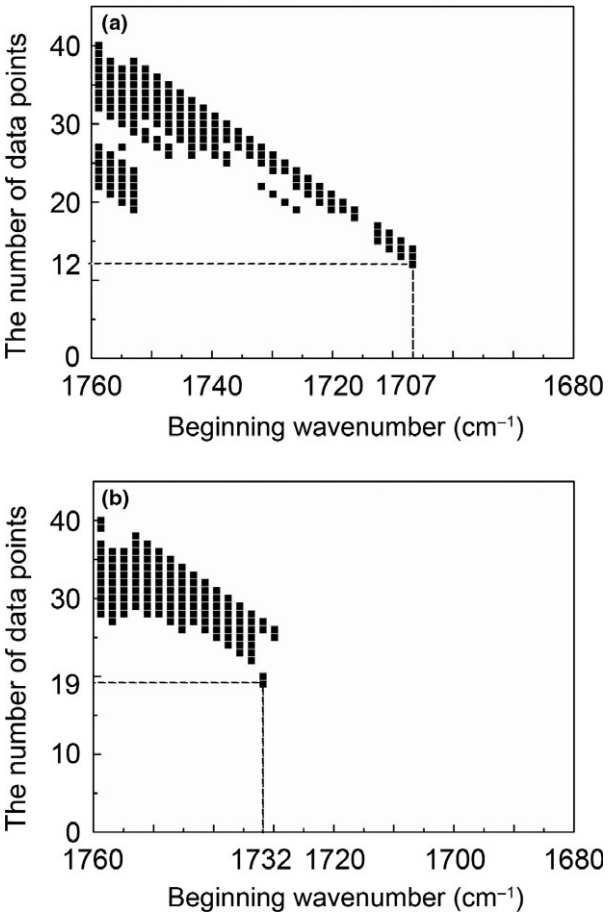

Figure 4 The number of spectral data points in LDFs developed in 165 windows for AFB1 (a) and LDFs developed in 126 windows for AFTs (b).

1710 cm^{-1} and the decreasing absorbance at 1743 cm^{-1} (Fig. 3a). $AR_{threshold}$ value of 13.05 was used in DF1 to screen forty AFB1-positive samples.

MWFDA was applied in the fingerprint region (forty-one data points in total). A total of 861 windows with size varying from 1 to 41 were used. LDFs developed in 165 windows could give 100% TPR and TNR (Fig. 4a). The OLDF developed in the narrowest window of 1707–1685 cm^{-1} (twelve data points) was used to be the DF2 for *C*2-node (Fig. 3b). With the setup of both DFs, the AFB1-MDT model could completely classify the contaminated oil samples. The calibration model applied to the validation set yielded 100% TPR and TNR (Fig. 3c, d).

AFTs-MDT model calibration and validation

The AFTs-MDT modelling and the resultant trend were very similar to those of AFB1. $AR_{threshold}$ was set to 13.05 in DF1, forty AFT-positive samples could be screened (Fig. 5a). LDFs for AFTs developed in 126 windows could give 100% TPR and TNR (Fig. 4b). The OLDF developed in the window of 1732–1697 cm^{-1} (nineteen data points) was the DF2 (Fig. 5b). With the setup of the both DFs, the AFTs-MDT model could completely classify the contaminated oil samples. The calibration model applied to the validation set also yielded 100% TPR and TNR (Fig. 5c, d).

Modification of discrimination function 2

The AFB1-MDT model was developed using fourteen different data points including two data points in DF1 and twelve data points in DF2. The AFTs-MDT model was developed using twenty different data points including two data points in DF1 and nineteen data points in DF2. The two models were optimal for the design of AFB1- and AFT-screening instruments, respectively.

The number of the total different data points in the two models was 30. Optimising the number of the total

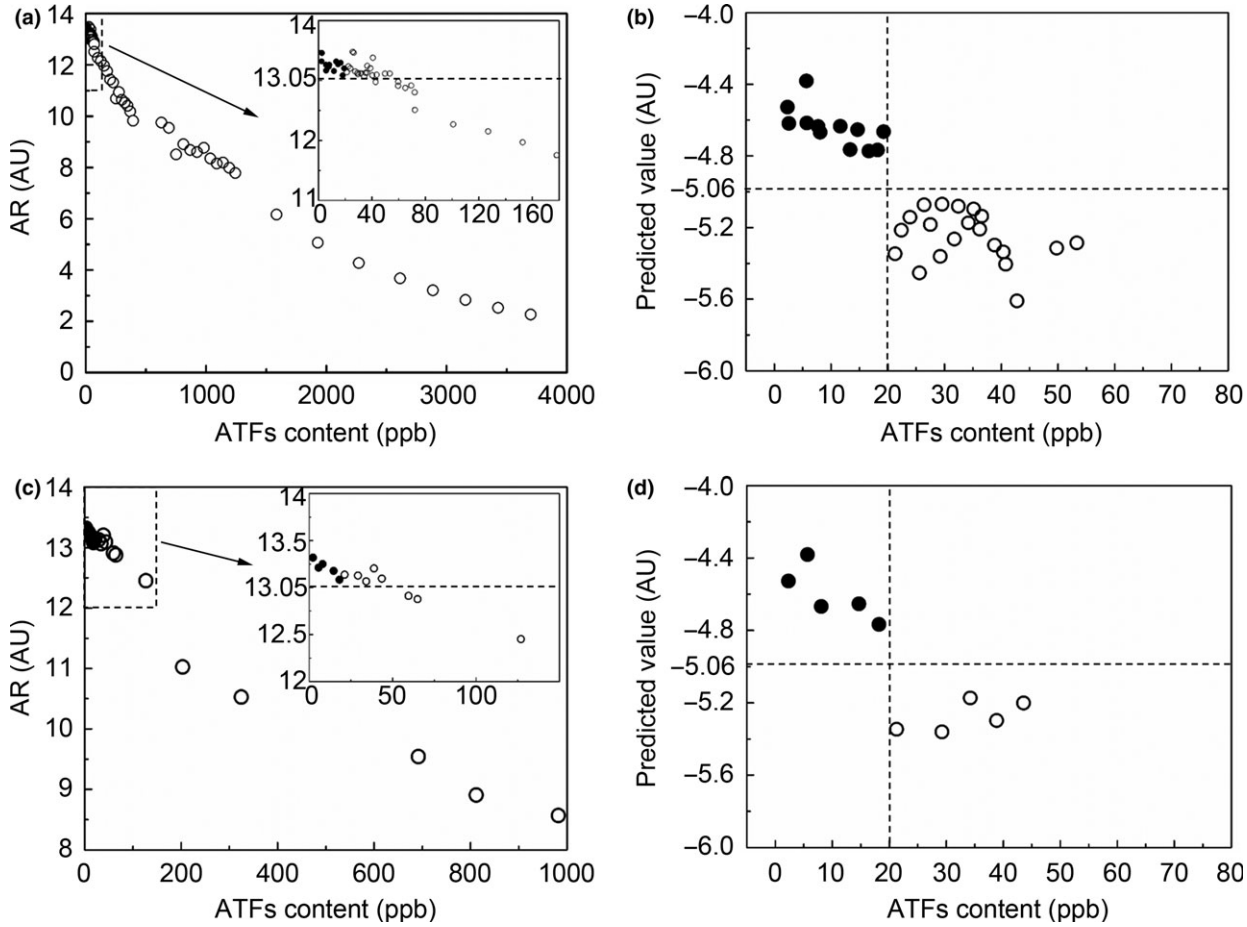

Figure 5 DF1 and DF2 classification results of MDT model in calibration (a and b) and validation (c and d) for AFTs. Positive samples denoted by open circles; negative samples denoted by filled circles.

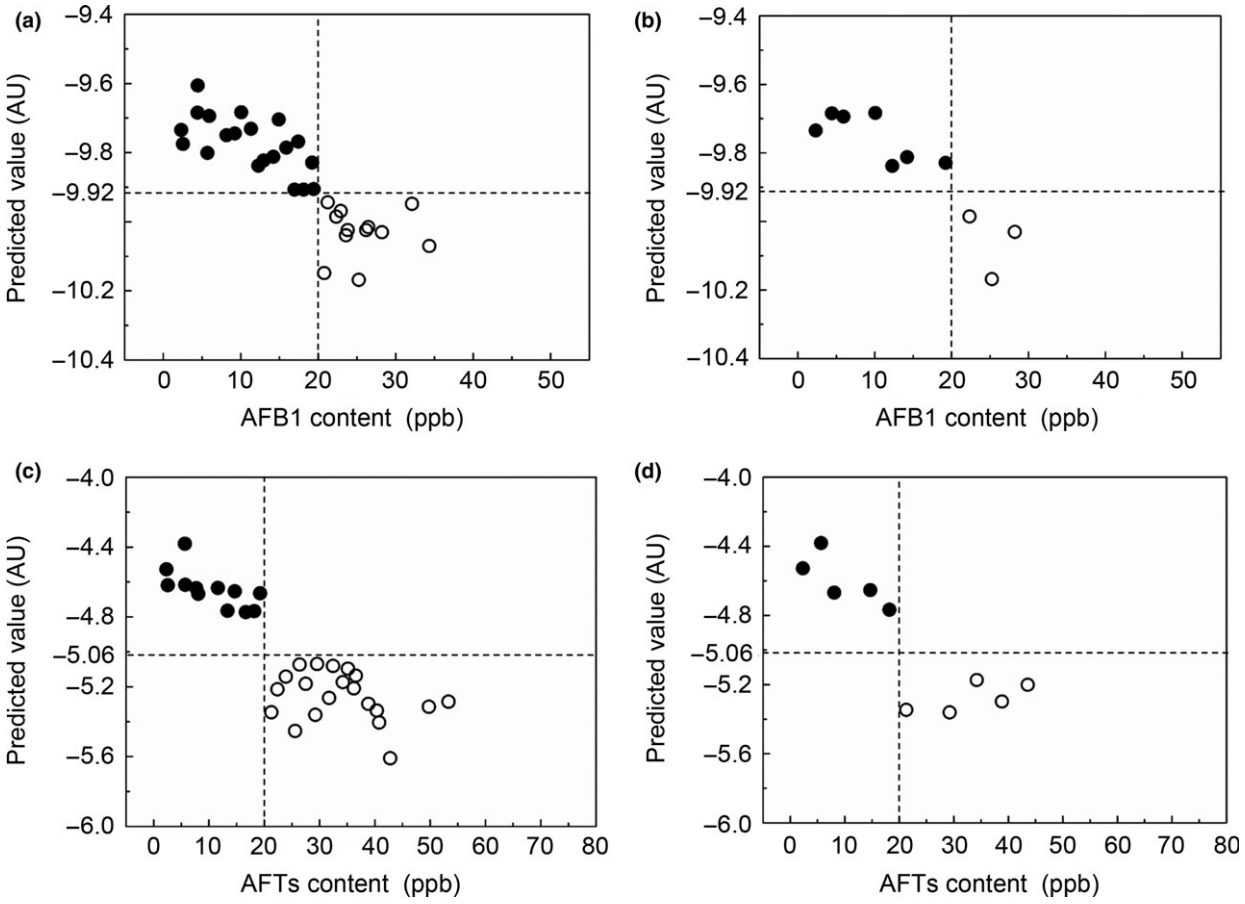

Figure 6 DF2 classification results in adjusted window in calibration (a) and validation (b) for AFB1. DF2 classification results in adjusted window in calibration (c) and validation (d) for AFTs. Positive samples denoted by open circles; negative samples denoted by filled circles.

different data points in the two models was necessary in the design of a multitasking instrument capable of simultaneously identifying AFB1- and AFT-positive samples. Further reduction in the total different data points was achieved by window adjustment on two DF2s in both models. The different data points in each of the 20 790 window combinations (126 × 165) of the two DF2s and the two different data points in DF1s were combined and compared to get the minimum number. The minimum number was twenty-three, including nineteen data points in DF2 in adjusted window for AFB1 (Fig. 6a, b), the nineteen data points in DF2 in adjusted window for AFTs (Fig. 6c, d) and four data points in both DF1s. The two DF2s modelled data points in adjusted windows 1726–1691 cm^{-1} and 1732–1697 cm^{-1} for AFB1 and AFTs, respectively.

Conclusions

A new analytical procedure, MIR spectra combined with a novel MDT method, successfully screened the contaminated peanut oil. AR and MWFDA methods were used to form DFs for complex nodes in the MDT models. TPR and TNR of two MDT models could both reach 100% in calibration and validation. Moving window and window adjustment techniques could reduce the total different data points to only twenty-three in two models. The MDT models with reduced number of data points in this study can be incorporated in the design of portable high-speed multitasking MIR instruments for screening AFT- and AFB1-positive peanut oil. The further studies of the applicability of models should be considered on a larger sample size to improve robustness.

Acknowledgment

This work was supported by the National Natural Science Foundation of China (No. 31101307, 6117 7075, 61275046, 61361166006, 61475066, 61405075, 61401176, 61505069, 61575084), Natural Science Foundation of Guangdong Province (No. 2014A030313377,

2014A030310205, 2015A030306046, 2015A030313320, 2016A030311019, 2016A030313079, 2016A030310098) and Science and Technology Projects of Guangdong Province (No. 2015A020213006, 2015B010125007, 2016B010111003, 2016A010101017).

Conflict of interest

There is no conflict of interest.

References

Ayres, J.L., Lee, D.J., Wales, J.H. & Sinnhuber, R.O. (1971). Aflatoxin structure and hepatocarcinogenicity in rainbow trout (Salmo gairdneri). *Journal of the National Cancer Institute*, **46**, 561–564.

Boutrif, E. (1998). Prevention of aflatoxin in pistachios. *Food, nutrition and agriculture*, **21**, 32–39.

Brereton, R.G. (2015). Pattern recognition in chemometrics. *Chemometrics & Intelligent Laboratory Systems*, **149**, 90–96.

Clifford, J.I. & Rees, K.R. (1967). The Action of aflatoxin B1 on the Rat Liver. *Biochemical Journal*, **102**, 65–75.

Daradimos, E., Marcaki, P. & Koupparis, M. (2000). Evaluation and validation of two fluorometric HPLC methods for the determination of aflatoxin B1 in olive oil. *Food Additives & Contaminants*, **17**, 65–73.

De Santis, B., Debegnach, F., Gregori, E. *et al.* (2017). Development of a LC-MS/MS method for the multi-mycotoxin determination in composite cereal-based samples. *Toxins*, **9**, 169–180.

Diniz, P.H.G.D., Gomes, A.A., Pistonesi, M.F., Band, B.S.F. & Araújo, M.C.U.D. (2014). Simultaneous classification of teas according to their varieties and geographical origins by using NIR spectroscopy and SPA-LDA. *Food Analytical Methods*, **7**, 1712–1718.

Durmuş, E., Güneş, A. & Kalkan, H. (2017). Detection of aflatoxin and surface mould contaminated figs by using Fourier transform near-infrared reflectance spectroscopy. *Journal of the Science of Food & Agriculture*, **97**, 317–323.

Fennema, O.R. (1997). Lipids. In: *Food Chemistry* (edited by O.R. Fennema). Pp. 261–264. New York: Marcel Dekker Inc.

Fernández-Ibañez, V., Soldado, A., Martínez-Fernández, A. & de la Roza-Delgado, B. (2009). Application of near infrared spectroscopy for rapid detection of aflatoxin B1 in maize and barley as analytical quality assessment. *Food Chemistry*, **113**, 629–634.

Guillén, M.D. & Cabo, N. (1997). Characterization of edible oils and lard by Fourier transform infrared spectroscopy. Relationships between composition and frequency of concrete bands in the fingerprint region. *Journal of the American Oil Chemists Society*, **74**, 1281–1286.

Holland, R.D. & Sepaniak, M.J. (1993). Qualitative analysis of mycotoxins using micellar electrokinetic capillary chromatography. *Analytical Chemistry*, **65**, 1140–1146.

Huang, F.R., Li, Y.P., Guo, H.X. *et al.* (2016). Identification of waste cooking oil and vegetable oil via Raman spectroscopy. *Journal of Raman Spectroscopy*, **47**, 860–864.

Kamiński, B., Jakubczyk, M. & Szufel, P. (2018). A framework for sensitivity analysis of decision trees. *Central European Journal of Operations Research*, **26**, 135–159.

Karunathilaka, S.R., Mossoba, M.M., Chung, J.K., Haile, E.A. & Srigley, C.T. (2017). Rapid prediction of fatty acid content in marine oil omega-3 dietary supplements using a portable fourier transform infrared (FTIR) device and partial least-squares regression (PLSR) analysis. *Journal of Agricultural & Food Chemistry*, **65**, 224–233.

Kaya-Celiker, H., Mallikarjunan, P.K., Schmale, D.G. & Christie, M.E. (2014). Discrimination of moldy peanuts with reference to aflatoxin using FTIR-ATR system. *Food Control*, **44**, 64–71.

Korani, W.A., Chu, Y., Holbrook, C., Clevenger, J. & Ozias-Akins, P. (2017). Genotypic regulation of aflatoxin accumulation but not aspergillus fungal growth upon post-harvest infection of peanut (Arachis hypogaea L.) seeds. *Toxins*, **9**, 218–229.

Lee, K.M., Davis, J., Herrman, T.J., Murray, S.C. & Deng, Y. (2015). An empirical evaluation of three vibrational spectroscopic methods for detection of aflatoxins in maize. *Food Chemistry*, **173**, 629–639.

Li, X.B., Sweigart, J.R., Teng, J.T.C., Donohue, J.M., Thombs, L.A. & Wang, S.M. (2003). Multivariate decision trees using linear discriminants and tabu search. *IEEE Transactions on Systems Man & Cybernetics Part A Systems & Humans*, **33**, 194–205.

Liu, R.J., Jin, Q.Z., Huang, J.H. *et al.* (2011). Photodegradation of Aflatoxin B_1 in peanut oil. *European Food Research & Technology*, **232**, 843–849.

Montgomery, D.C. (2013). Fitting regression models. In: *Design and Analysis of Experiments* (edited by D.C. Montgomery). Pp. 468–469. Hoboken, NJ: John Wiley & Sons Inc.

National Health and Family Planning Commission. (2016). GB 5009.22-2016: Determination of aflatoxins B1, B2, G1, G2 in foods (edited by China Food and Drug Administration). Pp. 1–7. Beijing, China: Standards Press of China.

National Health and Family Planning Commission. (2017). GB 2761-2017: Maximum levels of mycotoxins in foods (edited by China Food Drug Administration). Pp. 2–3. Beijing, China: Standards Press of China.

Pearson, T.C., Wicklow, D.T., Maghirang, E.B., Xie, F. & Dowell, F.E. (2001). Detecting aflatoxin in single corn kernels by transmittance and reflectance spectroscopy. *Transactions of the ASAE*, **44**, 1247–1254.

Pinto, R.C., Locquet, N., Eveleigh, L. & Rutledge, D.N. (2010). Preliminary studies on the mid-infrared analysis of edible oils by direct heating on an ATR diamond crystal. *Food Chemistry*, **120**, 1170–1177.

Ramos Catharino, R., de Azevedo Marques, L., Silva Santos, L. *et al.* (2005). Aflatoxin screening by MALDI-TOF mass spectrometry. *Analytical Chemistry*, **77**, 8155–8157.

Shen, F., Wu, Q.F., Tang, P.A., Shao, X.L. & Jiang, D.F. (2016). Attenuated total reflectance-fourier transform infrared spectroscopy (ATR-FTIR) for rapid detection of Aflatoxin B1 in brown rice. *Food Science*, **37**, 187–191.

Shigemasa, Y., Matsuura, H., Sashiwa, H. & Saimoto, H. (1996). Evaluation of different absorbance ratios from infrared spectroscopy for analyzing the degree of deacetylation in chitin. *International Journal of Biological Macromolecules*, **18**, 237–242.

Sinclair, R.G., Mckay, A.F. & Jones, R.N. (1952). The infrared absorption spectra of saturated fatty acids and esters[1]. *Journal of the American Chemical Society*, **74**, 2570–2575.

Tripathi, S. & Mishra, H.N. (2009). A rapid FT-NIR method for estimation of aflatoxin B1 in red chili powder. *Food Control*, **20**, 840–846.

United States Department of Agriculture (2017). Oilseeds: World Markets and Trade [Internet document]. Available from https://apps.fas.usda.gov/psdonline/circulars/oilseeds.pdf [Accessed 12/12/2017].

Yang, L., Ding, H., Gu, Z. *et al.* (2009). Selection of single chain fragment variables with direct coating of aflatoxin B1 to enzyme-linked immunosorbent assay plates. *Journal of Agricultural & Food Chemistry*, **57**, 8927–8932.

Zekavati, R., Safi, S., Hashemi, S. *et al.* (2013). Highly sensitive FRET-based fluorescence immunoassay for aflatoxin B1 using cadmium telluride quantum dots. *Microchimica Acta*, **180**, 1217–1223.

Zhang, Q., Jia, F.G., Liu, C.H., Sun, J.K. & Zheng, X.Z. (2014). Rapid detection of aflatoxin B1 in paddy rice as analytical quality assessment by near infrared spectroscopy. *International Journal of Agricultural & Biological Engineering*, **7**, 127–133.

Zweig, M.H. & Campbell, G. (1993). Receiver-operating characteristic (ROC) plots: a fundamental evaluation tool in clinical medicine. *Clinical Chemistry*, **39**, 561–577.